Research Article | Vol. 26, No. 15 | 23 Jul 2018 | OPTICS EXPRESS 18855
Optics EXPRESS

Broadband Fourier-transform coherent Raman spectroscopy with an ytterbium fiber laser

NICOLA COLUCCELLI,[1,2,*] EDOARDO VICENTINI,[1] ALESSIO GAMBETTA,[1,2] CHRISTOPHER R HOWLE,[3] KENNETH MCEWAN,[3] PAOLO LAPORTA,[1,2] AND GIANLUCA GALZERANO[1,2]

[1] *Dipartimento di Fisica, Politecnico di Milano, Piazza Leonardo da Vinci 32, 20133 Milano, Italy*
[2] *Istituto di Fotonica e Nanotecnologie - CNR, Piazza Leonardo da Vinci 32, 20133 Milano, Italy*
[3] *Defence Science and Technology Laboratory, Porton Down, Salisbury SP4 0JQ, UK*
[*] *nicola.coluccelli@polimi.it*

Abstract: We demonstrate a Fourier transform (FT) coherent anti-Stokes Raman scattering (CARS) spectroscopy system based on fiber technology with ultra-broad spectral coverage and high-sensitivity. A femtosecond ytterbium fiber oscillator is amplified and spectrally broadened in a photonic crystal fiber to synthesize pulses with energy of 14 nJ at 1040 nm, that are compressed to durations below 20 fs. The resulting pulse train is coupled to a FT-CARS interferometer enabling measurement of high-quality CARS spectra with Raman shifts of ~3000 cm^{-1} and signal to noise ratio up to 240 and 690 with acetonitrile and polystyrene samples, respectively, for observation times of 160 μs; a detection limit of one part per thousand is demonstrated with a cyanide/water solution. The system has the potential to detect trace contaminants in water as well as other broadband high-sensitivity CARS spectroscopy applications.

OCIS codes: (140.3510) Lasers, fiber; (320.0320) Ultrafast optics, supercontinuum generation; (300.6230) Spectroscopy, coherent anti-Stokes Raman scattering.

References and links

1. C. L. Evans, and X. S. Xie, "Coherent anti-Stokes Raman scattering microscopy: Chemical imaging for biology and medicine," Annu. Rev. Anal. Chem. **1,** 883–909 (2008)
2. D. Oron, N. Dudovich, and Y. Silberberg, "Femtosecond Phase-and-Polarization Control for Background-Free Coherent Anti-Stokes Raman Spectroscopy," Phys. Rev. Lett. **90,** 213902 (2003).
3. R. Selm, M. Winterhalder, A. Zumbusch, G. Krauss, T. Hanke, A. Sell, and A. Leitenstorfer, "Ultrabroadband background-free coherent anti-Stokes Raman scattering microscopy based on a compact Er:fiber laser system," Opt. Lett. **35,** 3282 (2010).
4. D. L. Marks, C. Vinegoni, J. S. Bredfeldt, and S. A. Boppart, "Interferometric differentiation between resonant coherent anti-Stokes Raman scattering and nonresonant four-wave-mixing processes," Appl. Phys. Lett. **35,** 5787 (2004).
5. N. Dudovich, D. Oron and Y. Silberberg, "Single-pulse coherently controlled nonlinear Raman spectroscopy and microscopy," Science **418,** 512 (2002).
6. F. Ganikhanov, C. L. Evans, B. G. Saar, and X. S. Xie, "High-sensitivity vibrational imaging with frequency modulation coherent anti-Stokes Raman scattering (FM CARS) microscopy," Opt. Lett. **31,** 1872 (2006).
7. C. H. Camp Jr, Y. J. Lee, J. M. Heddleston, C. M. Hartshorn, A. R. Hight Walker, J. N. Rich, J. D. Lathia, and M. T. Cicerone, "High-speed coherent Raman fingerprint imaging of biological tissues," Nature Photonics **8,** 627?634 (2014)
8. M. Cui, M. Joffre, J. Skodack, and J. P. Ogilvie, "Interferometric Fourier transform coherent anti-stokes Raman scattering," Opt. Express **35,** 8448 (2006).
9. K. Isobe, A. Suda, M. Tanaka, F. Kannari, H. Kawano, H. Mizuno, A. Miyawaki, and K. Midorikawa, "Fourier-transform spectroscopy combined with a 5-fs broadband pulse for multispectral nonlinear microscopy," Phys. Rev. A **77,** 063832 (2008).
10. T. Ideguchi, S. Holzner, B. Bernhardt, G. Guelachvili, N. Picqué and T. W. Hansch, "Coherent Raman spectro-imaging with laser frequency combs," Nature **502,** 355 (2013)
11. M. Tamamitsu, Y. Sakaki, T. Nakamura, G. K. Podagatlapalli, T. Ideguchi, and K. Goda "Ultrafast broadband Fourier-transform CARS spectroscopy at 50000 spectra/s enabled by a scanning Fourier-domain delay line," Vib. Spectrosc. **91,** 163 (2017)

#332157 https://doi.org/10.1364/OE.26.018855
Journal © 2018 Received 21 May 2018; accepted 21 Jun 2018; published 9 Jul 2018

Optics EXPRESS

12. K. Hashimoto, M. Takahashi, T. Ideguchi, and K. Goda, "Broadband coherent Raman spectroscopy running at 24000 spectra per second," Sci. Rep. **6,** 21036 (2016)
13. K. J. Mohler, B. J. Bohn, M. Yan, G. Melen, T. W. Hansch, and N. Picqué, "Dual-comb coherent Raman spectroscopy with lasers of 1-GHz pulse repetition frequency," Opt. Lett. **42,** 318 (2017)
14. N. Coluccelli, C. R. Howle, K. McEwan, Y. Wang, T. T. Fernandez, A. Gambetta, P. Laporta, and G. Galzerano, "Fiber-format dual-comb coherent Raman spectrometer," Opt. Lett. **42,** 4683 (2017)
15. S. R. Domingue, and R. A. Bartels, "Overcoming temporal polarization instabilities from the latent birefringence in all-normal dispersion, wave-breaking-extended nonlinear fiber supercontinuum generation," Opt. Express **21,** 13305 (2013)
16. H. Tu, Y. Liu, J. Laegsgaard, U. Sharma, M. Siegel, D. Kopf, and S. A. Boppart, "Scalar generalized nonlinear Schrodinger equation-quantified continuum generation in an all-normal dispersion photonic crystal fiber for broadband coherent optical sources," Opt. Express **18,** 27872 (2010)
17. D. M. Riffe and A. J. Sabbah, "A compact rotating-mirror autocorrelator design for femtosecond and picosecond laser pulses," Rev. Sci. Instrum. **69,** 3099 (1998)
18. K. Hiramatsu, Y. Luo, T. Ideguchi, and K. Goda, "Rapid-scan Fourier-transform coherent anti-Stokes Raman scattering spectroscopy with heterodyne detection," Opt. Lett. **42,** 4335–4338 (2017)

1. Introduction

Coherent Raman spectroscopy has been widely recognized as an excellent tool for observation of molecule vibrations, providing identification of chemical species in different applications of biophysics, biology, food analysis, and more generally analytical chemistry [1]. In this context, broadband coherent anti-Stokes Raman scattering spectroscopy is very attractive, as it combines the acquisition speed enabled by the coherent excitation to the multispectral information capability that is required for molecular fingerprinting. Several CARS detection techniques have been reported so far, working both in frequency and time domains, including coherent control CARS [2], time-resolved CARS [3], interferometric CARS [4], single-pulse CARS [5], frequency-modulation CARS (FM-CARS) [6] and multiplex CARS [7]. Besides these, Fourier-transform CARS (FT-CARS) [8, 9] has been used as a time domain technique, featuring complete non-resonant background cancellation, resolution limited by the time span of the FT window, and broadband acquisition with a single detector. Fourier transform CARS, including also the modality called dual-comb CARS [10], is based on generating interferences between replicate pairs of blue-shifted anti-Stokes (or red-shifted Stokes) pulses as a function of time delay between replicas, and transforming the resulting interferogram to obtain the Raman spectrum of molecules. The relevant FT-CARS system reported so far are based on Ti:sapphire lasers to take advantage of the broadband pulses with typical energy of 0.5-3 nJ and Raman span of 200-1400 cm^{-1}; the potential for fast acquisition rates has also been demonstrated to improve the sensitivity by averaging [11–13]. A proof-of-concept fiber-format dual-comb CARS system has also been demonstrated [14], however, apart from the need for two femtosecond oscillators, a common issue to all dual-comb spectroscopy setups, this system was limited by the relative frequency jitter of the two combs and the power available for CARS excitation, which reduced the performance in terms of resolution and sensitivity.

In this letter, we report on a FT-CARS spectroscopy system based on using a single high-power Yb-fiber source coupled to a FT interferometer, which is intrinsically immune to the problem of relative frequency jitter and enables measurement of CARS spectra with exceptionally high signal-to-noise ratio; moreover, we extended the range of accessible Raman shifts up to 3000 cm^{-1}, allowing for observation of H-stretch (>2500 cm^{-1}), and CN, CO, CC double/triple covalent bonds (1500-2500 cm^{-1}), as well as the whole fingerprint region (0-1500 cm^{-1}). In particular, we observed CARS spectra of liquid acetonitrile and polystyrene film with signal-to-noise ratio of 240 and 690, respectively, on single interferogram acquisition with duration of 160 μs; additionally, using a solution of acetonitrile/water, we demonstrated a detection sensitivity of 10^{-3} against cyanide (CN^-) contamination, by averaging over 500 spectra.

The experimental layout adopted during FT-CARS experiments is shown in Fig. 1. The system

Optics EXPRESS

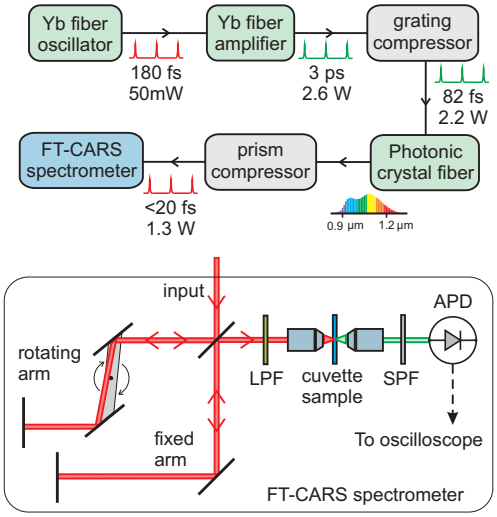

Fig. 1. Layout of the FT-CARS system with detail of the interferometer and coherent Raman excitation and detection unit. LPF, long-pass filter; SPF, short-pass filter; APD, avalanche photodiode

is based upon a femtosecond Yb-fiber ring oscillator generating pure solitons with duration of 180 fs at a repetition frequency of 94 MHz, and an average output power of 50 mW (pulse energy of ~0.5 nJ). As solitonic oscillators cannot be operated at high power due to the onset of multiple pulsing, a femtosecond Yb-fiber amplifier has been implemented. Prior to amplification, the pulses are stretched in a HI1060 fiber with a length of 2 m, and then sent through a hybrid WDM for multiplexing with the amplifier pump diode. The pump diode has a maximum output power of 30 W at 960 nm and is coupled to a multimode fiber with a diameter of 125 μm. The output fiber of the WDM is spliced to the amplifier fiber, an Yb-doped double-clad fiber with core/cladding diameter of 20/128 μm and length of 2 m. At this point, the pulse train has average power 2.6 W and pulse duration ~3 ps. A grating compressor allows for pulse compression down to 82 fs, with a resulting average power of 2.2 W. Figure 2(a), (b) shows the spectrum and autocorrelation trace

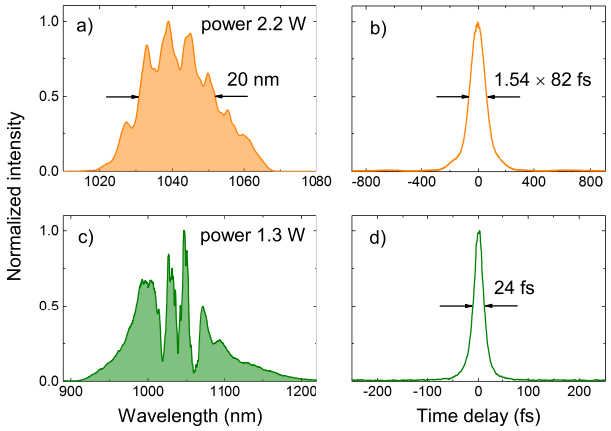

Fig. 2. Spectra (a,c) and autocorrelations (b,d) of pulses generated by the Yb-fiber amplifier (orange lines) and LMA-PCF (green lines).

Optics EXPRESS

of the amplified pulses after the grating compressor. The pump diode has been limited to power levels below 6 W; at higher pump power, the pulse duration increases due to the onset of fiber nonlinearities which are not compensated by the grating compressor, and are detrimental to the subsequent supercontinuum generation.

After amplification and compression, the pulses are coupled into 6-cm length polarization maintaining (PM) large mode area (LMA) photonic crystal fiber (PCF, NKT Photonics LMA-PM-10), where strong spectral broadening mainly due to self-phase modulation occurs. This fiber has a core diameter of 10 μm, larger than previously reported [14], to ensure a stable input coupling at high power, and to provide a normal dispersion in the relevant wavelength regime thereby achieving a recompressible phase distribution [15, 16]; additionally, the PM feature reduces depolarization noise during supercontinuum generation, which typically degrades the coherence and prevents the synthesis of ultrashort pulses [16]. Input and output coupling is achieved using two aspheric lenses with focal length of 7.5 mm. The dispersion of the LMA-PCF (~500 fs^2/mm) has been compensated using an SF10 prism compressor. Figure 2(c), (d) shows the resulting spectrum and autocorrelation trace of pulses after the prism compressor. As the autocorrelation trace has a duration of 24 fs, the pulse duration is assumed to be less than 20 fs. The spectrum of the supercontinuum spans the spectral range from 910 nm to 1220 nm and with 1.3 W of average power and an intensity-noise standard deviation of 1% over one hour.

The high-power sub-20-fs pulses are coupled into a home-made Michelson interferometer consisting of a fixed and a rotating arm with equalized dispersions, which allows for generation of CARS spectra with the same spectral extension. In particular, at the short pump pulse durations adopted here, any small unbalancing of dispersions gives non-optimized pulse durations along one arm which prevents exploitation of the full span of Raman frequencies enabled by the available pulse bandwidth. The rotating arm of the interferometer consists of two 45° mirrors mounted on a 6-cm long rotating bracket allowing for scanning the delay between pulses in the two arms while preserving high linearity of delay as a function of time [17]. Note that, the linearity of delay affects the resolution of the instrument, and previous FT-CARS interferometers based on rotating optics (polygonal or galvo mirrors) have shown very high nonlinearity of delay that could be only compensated in real-time or post-processing by an additional continuous-wave laser for tracking the delay as a function of time [11, 12]. On the other side, interferometer design based on scanning linear stages shows high linearity of delay but low scanning speed, and the resulting Raman spectrum is typically detected at Fourier frequencies below few hundreds kilohertz, where most of the intensity noise of the CARS signal is located, limiting the sensitivity

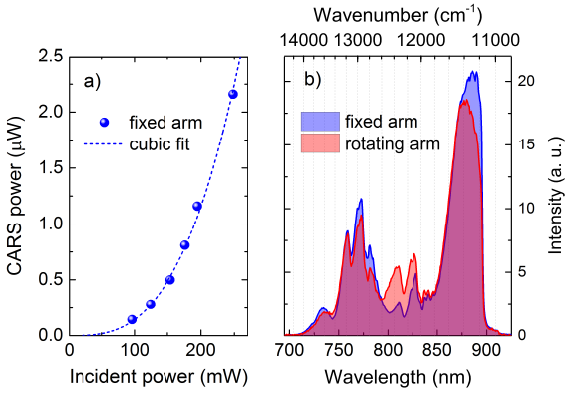

Fig. 3. a) Average power of CARS beam as a function of power incident onto the acetonitrile sample (beam in the rotating arm blocked). b) Spectrum of CARS radiation generated by pulses in the fixed (blue line) and rotating (red line) arm of the interferometer.

Optics EXPRESS

of the system. The design of the interferometer adopted here is characterized by high linearity of delay as a function of time, resulting in a resolution limited only by the amount of delay used for FT, and fast scanning of delay, which maps the Raman spectrum at Fourier frequencies below few megahertz, where noise from the source is absent and the limit to sensitivity is only dependent upon the shot noise.

The pulse replicas propagating along the interferometer are recombined through a beam splitter (Thorlabs, UFBS5050) and then filtered by a long-pass filter (LPF, Thorlabs FELH0900) with wavelength cutoff at 900 nm. An achromatic lens with focal length of 7.5 mm focuses the pulses

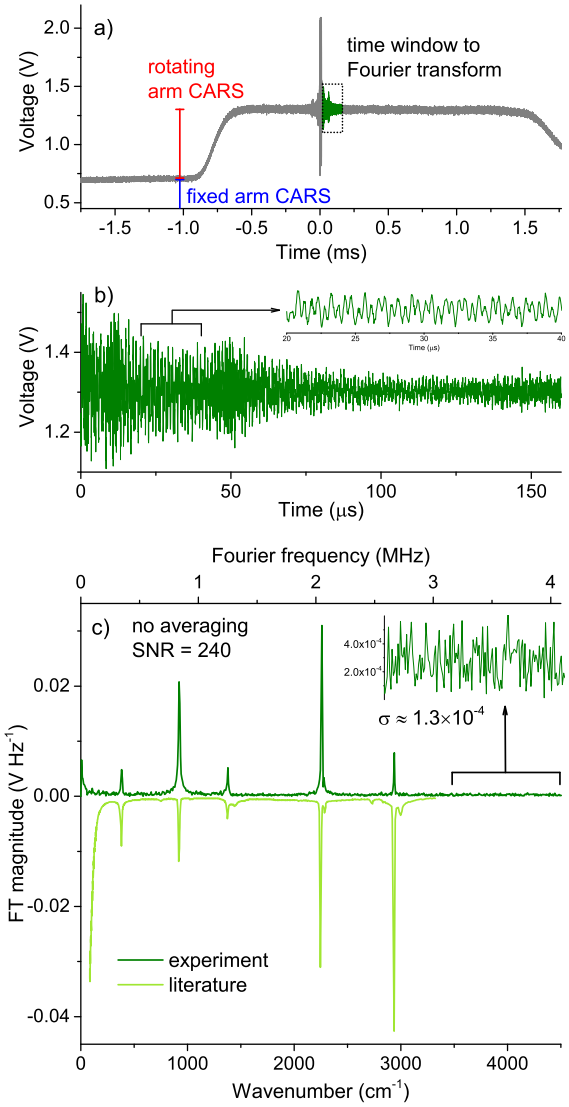

Fig. 4. a) Typical oscilloscope trace showing equalized CARS contributions from the fixed and rotating interferometer arms, and interferogram with large non-resonant background around zero delay followed (and preceded) by the Raman relaxation signal. b) Detail of the 160-μs time window selected for FT calculation. c) Background-free CARS spectrum calculated by FT of one interferogram (top), and reference spectrum (bottom), of pure acetonitrile. The inset shows the detail of noise floor.

Optics EXPRESS

on a liquid sample of acetonitrile within a 2-mm long cuvette and the resulting CARS beam is collected onto a Si avalanche photodiode (APD, 10-MHz band, Thorlabs APD410A2) by a similar lens; the pump is blocked by a short-pass filter (SPF, Thorlabs FESH0900) with cutoff at 900 nm. The signal generated by the APD is then digitized using a 12-bit oscilloscope with a sampling rate of 50 MS/s and processed for proper time windowing and FT calculation. Figure 3 shows the CARS beam power as a function of incident pump power along with a cubic fitting. A CARS power in excess of 2 μW has been observed at incident power level of 250 mW (pulse energy of 2.6 nJ), sufficiently high to drive the APD to saturation. Additionally, Figure 3 shows CARS spectra generated by pulses propagating through the two interferometer arms as measured by a Si array spectrometer. As a consequence of dispersion equalization, the CARS spectra are similar, and in particular their spectral extension from 700 to 900 nm (~3000 cm^{-1}) is the same, as required for a full exploitation of the Raman band enabled by the light source developed here.

Figure 4 shows a typical temporal trace and the resulting spectrum acquired with the FT-CARS setup. The acquisition rate is 100 spectra/s, limited by maximum angular velocity of the rotating arm. The fixed-arm pulses give a constant CARS contribution, while the rotating-arm pulses contribute only within a limited time window of ~2.5 ms, specifically when the rotation angle allows back-reflection to the sample, corresponding to a delay scan of ~30 ps. The interferogram occurs when the pulse replicas overlap, and consists of a long tail of CARS oscillations and a strong impulsive non-resonant background. The relevant signal is selected by a rectangular window with duration of 160 μs, corresponding to a resolution of 4 cm^{-1}. The FT is shown in Fig.4(c) and represents the CARS spectrum of pure acetonitrile. The average power of pulses from both interferometer arms is 250 mW (pulse energy of 2.6 nJ). The span of Raman shifts extends from 300 to 3000 cm^{-1} and the signal-to-noise ratio (SNR) is 240 on the main peak at 2253 cm^{-1}, using one interferogram. Overall, the quality of the spectrum is very high, non-resonant background is totally removed and all relevant vibrations are precisely detected, including the stretch of cyanide and hydrogen at 2253 and 2943 cm^{-1}, thanks to the ultra broadband source developed here. The reduced amplitude of the peak at 382 cm^{-1} with respect to the reference spectrum (also shown in Fig. 4(c) is intrinsic to the detection technique as only a small part of low-frequency anti-Stokes power can pass the LPF and contributes to detection. Similarly, the sensitivity at high Raman frequency close to 3000 cm^{-1} is limited by the reduced power in the comb wings exciting high-frequency vibrations. As averaging allows for improvement of sensitivity, Fig. 5 shows the CARS spectrum of acetonitrile resulting from the average of 100 consecutive spectra, corresponding to a total acquisition time of 1 s; it is worth noting the SNR observed here of 2360 on the peak at 2253 cm^{-1}, and the unaffected width of the spectral lines, as a consequence of the common mode frequency jitter between pulse replicas, in contrast to previous results with fiber-based dual-comb CARS [14].

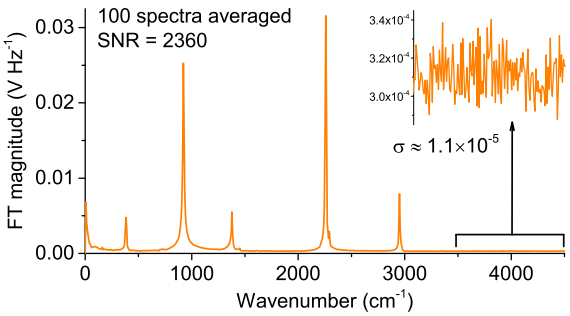

Fig. 5. CARS spectrum of pure acetonitrile as obtained by averaging over 100 consecutive spectra. The inset shows the detail of noise floor.

Optics EXPRESS

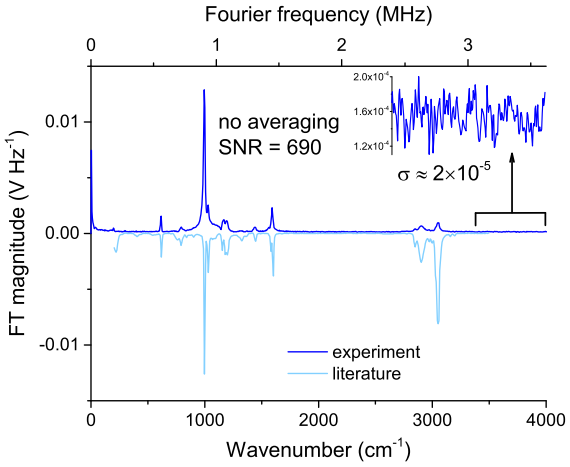

Fig. 6. Background-free CARS spectrum calculated by FT of a single interferogram (top), and reference spectrum (bottom), of an 80-μm thick polystyrene film. The inset shows the detail of noise floor.

As a further test, the FT-CARS spectrum of an 80-μm thick film of solid polystyrene has been measured. The test explores the potential of the system for microscopy applications, where low power are typically required by biological samples and spatial resolution is of primary importance. To this purpose, a variable neutral density filter has been placed before the LPF to reduce the average power of pulses from both interferometer arms to 20 mW (pulse energy of 0.2 nJ). Additionally, the focusing lens before the sample has been substituted by a 20X achromatic objective with numerical aperture of 0.65. Figure 6 shows the CARS spectrum of polystyrene in the Raman range from 300 to 3000 cm^{-1} with a SNR of 690 on the main peak at 998 cm^{-1}, using a single interferogram acquisition with a time duration of 160 μs. Notably, the SNR observed here is higher then acetonitrile because of different focusing optics yielding higher intensity in the focus, and a stronger resonance at 998 cm^{-1} with respect to the cyanide resonance at 2253 cm^{-1}. In particular, the beam radius in the focus is calculated to be a factor ~3 smaller then the focusing achromatic lens used for acetonitrile, corresponding to a factor ~10 in terms of intensity, which accounts for a similar overall resulting intensity in the focus, even though the incident power is different with respect to acetonitrile.

Finally, the potential of the system for detection of trace contaminants in water has been tested

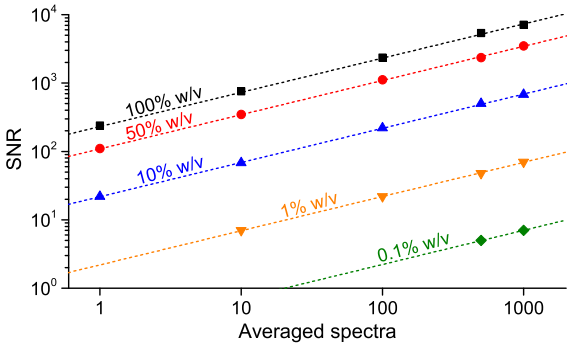

Fig. 7. Signal-to-noise ratio as a function of the number of averaged spectra calculated on the cyanide resonance at 2253 cm^{-1}, for different concentrations of cyanide diluted in water.

Optics EXPRESS

using a solution of water/acetonitrile, where the contaminant of interest is cyanide (CN^-). Figure 7 shows the SNR observed on the Raman peak of cyanide at 2253 cm^{-1} as a function of the number of averaged spectra, at different cyanide concentrations expressed in % w/v. As expected, the SNR increases as the square root of the number of averaged spectra. The dependence on concentration is explained on the basis of homodyne CARS detection theory, where the CARS signal is homodyned by an internal local oscillator represented by the non-resonant background, in contrast to heterodyne CARS, where the CARS signal is heterodyned by the residual of the probe pulse after filtering by the LPF [18]. Here, the power content of probe pulses at wavelength shorter then 900 nm (cutoff wavelength of LPF and SPF) is measured to be ~120 nW after the SPF (sample out of focus to avoid CARS emission), hence it is negligible with respect to CARS power, and homodyne CARS detection theory applies. According to this, the dependence of SNR with concentration is linear at low concentrations due to the predominant non-resonant background from water with respect to the CARS signal from cyanide molecules, and nonlinear at high concentration where the CARS contribution is stronger [18]. In the best case, a SNR of 5 has been observed at cyanide concentrations of 10^{-3} w/v by averaging over 500 spectra, corresponding to an observation time of 5 s. The sensitivity could be further scaled by increasing the power level of the pump, which gives cubic gain to CARS generation, or by implementing a balanced detection scheme.

2. Conclusion

In conclusion, a FT-CARS spectrometer with unprecedented spectral coverage and sensitivity has been demonstrated using a high-power Yb-fiber laser source. High-quality CARS spectra of acetonitrile and polystyrene have been measured in the Raman range from 300 to 3000 cm^{-1} at SNR of 240 and 690, respectively, with an observation time of 160 μs. A detection limit for cyanide contamination in water of one part per thousand has been demonstrated. Application of the system to microscopy experiments would require further development to avoid the dead time of around 10 ms between consecutive interferograms which presently limits the acquisition time. Being based on fiber technology, the system is very promising for "in field" applications of analytical chemistry, particularly the detection of trace contaminants in water, where any kind of chemicals can be detected exploiting the ultra-broad band and sensitive detection enabled by this approach.

Funding

DSTL Enduring Challange (CDE100909), UK Ministry of Defence, contract number DSTLX-1000107010.

Disclosures

The authors declare that there are no conflicts of interest related to this article.